

RAC1/miR-3613/RAC1 feedback loop contributes to ovarian cancer progression

Changzhong Li (✉ 15168888909@163.com)

Shandong University Affiliated Hospital: Shandong Provincial Hospital

Ruobing Leng

Shandong University Affiliated Hospital: Shandong Provincial Hospital

Yunfang Meng

Shandong University Affiliated Hospital: Shandong Provincial Hospital

Na Li

Shandong University Affiliated Hospital: Shandong Provincial Hospital

Feifei Li

Shandong University Affiliated Hospital: Shandong Provincial Hospital

Yingzi Zhao

Shandong University Affiliated Hospital: Shandong Provincial Hospital

Research Article

Keywords: RAC1, miR-3613, Ovarian cancer, Epithelial mesenchymal transition

Posted Date: April 8th, 2021

DOI: <https://doi.org/10.21203/rs.3.rs-380396/v1>

License:  This work is licensed under a Creative Commons Attribution 4.0 International License.

[Read Full License](#)

Abstract

The RAC1 signal pathway is involved in various tumor cell biological processes. Here, the role of RAC1-miR-3613-RAC1 negative feedback loop in ovarian cancer was explored. Results showed that RAC1 knockdown up-regulated miR-3613, which in turn inhibited RAC1 expression. RAC1 counteracted the inhibitory effect of miR-3613 on the proliferation and invasion of ovarian cancer cells in vitro and on the tumor growth in vivo. In ovarian cancer, miR-3613 expression was negatively correlated with RAC1, and patients with low miR-3613 expression had poor prognosis. These findings indicate the role of RAC1-miR-3613-RAC1 negative feedback loop in the malignant progression of ovarian cancer and its possible therapeutic values.

Introduction

Ovarian cancer is one of the malignant tumors with the highest incidence in women. Its most common type is epithelial ovarian cancer (EOC), which has the leading mortality rate among gynecological tumors and thus seriously threatens women's lives[1, 2]. The mainstream treatment of ovarian cancer is surgery to minimize the tumor burden, followed by chemotherapy to kill as many residual cancer cells as possible. However, many patients cannot tolerate the pain of chemotherapy[3]. In the era of molecular targeted therapy, people aim to extend the time from disease recurrence to death or the time interval to achieve a progress-free status; although the use of latest drugs bevacizumab and olaparib can delay this cancer progression, the opportunity to extend the lives of patients is still limited[4, 5].

The abnormal expression of cancer-related genes renders current anticancer therapies less effective or even ineffective. Rho-GTPases RhoA, RAC1, and Cdc42 are important regulators of cytoskeletal dynamics. Although many in vitro and in vivo experiments indicated the pro-tumor effects of activated Rho-GTPase, some of its tumor suppressor functions have also been described[6, 7]. Small GTPase is a molecular switch that alternates between the active GTP binding state and the inactive GDP binding state and regulates almost all aspects of cell biology through a series of complex and dynamic biochemical signal networks. RAC1 was first described as promoting phagocytosis by activating NADPH and producing superoxide and growth factors to form membrane folds through actin polymerization[8, 9]. Since then, RAC1 has been found to participate in various cellular processes, such as cell-matrix adhesion, migration, invasion, and proliferation[10-12]. Some studies confirmed the existence of nuclear RAC1 and revealed the mechanism that promotes RAC1 nuclear localization and its functional implications. For example, RAC1 directly interacts with BCA3 to promote nuclear NF-kB signaling[13]. Nuclear RAC1 directly interacts with nuclear phosphorus 1 (NPM1), which limits the GTP load of RAC1 and reduces cell proliferation[14].

On the one hand, miR-3613 binds to RAC1 mRNA to inhibit its translation. On the other hand, RAC1 inhibits the transcription of miR-3613 to relieve the inhibiting effect of the latter on the expression of the former and promote tumor progression to the greatest extent. This research enhances the understanding

on the biological mechanism of RAC1 in tumors and may provide certain theoretical support for the development of anti-tumor drugs targeting RAC1.

Materials And Methods

MicroRNA array

SKOV3 cells were transfected with RAC1 siRNA or siRNA NC. Total RNA was then isolated by TRIzol reagent (Takara, Japan) in accordance with the manufacturer's instructions. RNA quality was determined by a spectrophotometer at 260 and 280 nm, and RNA integrity was evaluated by 1.5% formaldehyde denaturing gel. Flash Tag Biotin HSR labeling was performed. Biotin-labeled RNA was hybridized to the Affymetrix GeneChip miRNA 4.0 Array (Affymetrix, Santa Clara, CA, USA). Transcriptome Analysis Console (Affymetrix, USA) was used to analyze differentially expressed miRNAs.

Cells and clinical specimens

Ovarian cancer cell lines SKOV3 and OVCAR3 were obtained from the Cell Resource Center of Chinese Academy of Medical Sciences and maintained in RPMI-1640 medium (Gibco, USA) supplemented with 10% FBS (Gibco, USA) and 1% penicillin–streptomycin solution (Beyotime, China) in a 5% CO₂ humidified incubator at 37 °C. Fresh tumor tissues and adjacent normal tissues were collected immediately after surgery in Shandong Provincial Hospital Affiliated to Shandong First Medical University. A written informed consent was obtained from each patient. Ethical approval from the Shandong Provincial Hospital Affiliated to Shandong First Medical University was received before the studies were performed in accordance with the Declaration of Helsinki.

qRT-PCR

The total RNA of the cells was extracted with Trizol (Sigma, USA) in accordance with the instructions. After quantification, 2 ug of RNA was used for reverse transcription with miR-3613 specific reverse transcription primers to obtain cDNA. The PCR primers of miR-3613 were then employed for amplification and quantification using the 2- $\Delta\Delta$ ct method. U6 snRNA was applied as the control. The primer sequences were as follows: miR-3613-5p-RT, 5'-GTCGTATCCAGTGCAGGGTCCGAGGTGCACTGGATACGACAACAAA-3', miR-3613-5p-forward, 5'-TGCGGTGTTG TACTTTTTTTTTT-3', miR-3613-5p-reverse, 5'-CCAGTGCAGGGTCCGAGGT-3', U6-RT, 5'-GTCGTATCCAGTGCAGGGTCCGAGGTGCACTGGATACGACAAAATATGGAAC-3', U6- forward, 5'-TGCGGGTGTCTCGCTTCGGCAGC-3', and U6- reverse, 5'-CCAGTGCAGGGTCCGA GGT-3'. Each experiment was performed in triplicate.

MTT

The cells were resuspended in a culture medium containing 10% FBS and inoculated in a 96-well plate with 1,000 cells per well. After 24 hours, lipofectamin3000 was used to transfect miRNA mimics and DNA plasmids into the cells, which were then cultured for 4 days. After transfection, cell viability was detected

by MTT method every day. Each well was added with 20 ul of 5 mg/ml MTT solution (Beyotime, China). After incubation for 4 hours, the medium was discarded, 150 ul of DMSO was added, and the mixture was shaken for 10 minutes. The absorption value of each hole was measured at a wavelength of 450 nm. Each experiment was performed in triplicate.

Colony formation assay

The cells in the logarithmic growth phase were digested with 0.25% trypsin and pipetted into single cells. The cells suspended in culture medium containing 2% FBS were seeded into a six-well plate at a density of 1000 cells per well. All cells were maintained in an incubator containing 5% CO₂ at 37 °C. The medium was changed every 3 days until visible clones were detected. Afterward, the medium was discarded, and the cells were carefully washed twice with PBS, fixed with 4% paraformaldehyde for 15 minutes, stained with GIMSA for 10–30 minutes, and slowly washed with running water. Images were capture to record the number of clones. Each experiment was performed in triplicate.

Wound healing

Approximately 5×10^5 cells were seeded in a 24-well plate and culture for 24 hours until the cell density was more than 90%. A10 ul pipette tip was then used to make a straight scratch. The cells were washed three times with PBS to remove the suspended cells. A serum-free medium was added, and the cells were placed in a 37 °C 5% CO₂ incubator for culture. After 24 hours, images were captured under a microscope, and the cell migration rate was calculated. Each experiment was performed in triplicate.

Transwell assay

In brief, 5 µg/µl Matrigel (BD, USA) was added to the upper chamber (Corning, USA) and placed at 37 °C for 30 min. The digested cells were washed with PBS, resuspended in a serum-free medium containing BSA, and seeded at a concentration of 10^5 per well. The lower chamber was added with 500 ul of medium containing 10% fetal bovine serum and cultured for 24 hours. The medium was then discarded, and the cells in the chamber were removed and fixed with 90% alcohol at room temperature for 30 minutes. The cells were then stained with 0.1% crystal violet at room temperature for 10 minutes. After being washed with water, the invasive cells were recorded under a microscope (Olympus, DP50, Japan). Each experiment was performed in triplicate.

Western blot

The total protein of the cells was harvested with RIPA lysate (Beyotime, China), quantified by BCA method, and then separated by 10% SDS-PAGE. The separated protein was transferred to the PVDF membrane. After being washed three times with TBST, the membrane was blocked in 5% BSA overnight at 4 °C and then incubated with the following diluted primary antibody for 2 hours at room temperature: RAC1 polyclonal antibody (Abcam, ab155938, UK), N-cadherin polyclonal antibody (Affinity, AF4039, China), vimentin polyclonal antibody (Affinity, AF7013, China), and GAPDH polyclonal antibody (Affinity,

AF0911, China). HRP-labeled secondary antibody was then added to react at room temperature for 2 hours, and the specimens were finally visualized by ECL luminescence reagent (Beyotime, China) until the protein is clear. Each experiment was performed in triplicate.

Plasmid, oligo, and transfection

Pre-miR-3613 genomic sequence was synthesized and inserted into pcDNA3.1 vector to construct the miR-3613 expression plasmid. RAC1 expression plasmid was purchased from SinoBiological Inc. (HG10535-CF). RAC1 siRNA sequence was 5'-CAAACAGUUGGAGA AACGUACGGUA-3'.

Luciferase activity assay

The wild type and mutant 3'-UTR of RAC1 were synthesized and cloned into the pmirGLO vector. The cells were seeded into a 48-well plate. After 24 hours, the luciferase reporter plasmids were transfected when the cell density reached approximately 70%. After 48 hours, the culture medium was discarded, and the cells were washed with 100 μ l of PBS. Each well was then added with 50 μ l of diluted lysis buffer and then shaken for 20 minutes on a shaker to ensure that the cells were completely lysed. Firefly luciferase and renilla luciferase activities were detected following the instructions of Dual-Lumi™ dual luciferase reporter gene detection kit (Beyotime, China). Each experiment was performed in triplicate.

In vivo experiments

Eighteen 5-week-old female BALB/c nude mice were purchased from Charles River Laboratories, Inc. and randomly classified into three groups, namely, vector control, miR-3613 overexpression group, and miR-3613 and RAC1 overexpression group. The prepared cells were injected subcutaneously into the nude mice at a concentration of 5×10^6 cells per mouse. Tumor volumes were monitored every 3 days. After 1 month, all animals were euthanized through the intravenous injection of sodium pentobarbital at a final concentration of 100 mg/kg. The surgically harvested solid tumor tissues were fixed in 4% formalin, and their volume was calculated as follows: $\text{volume} = (\text{length} \times \text{width}^2) / 2$. All the animals were well taken care of, and all the experiments were performed in accordance with the ethical standards of the Institutional Animal Use and Care Committee of the Shandong Provincial Hospital Affiliated to Shandong First Medical University. Ethical approval was obtained prior to the study. Each experiment was performed in triplicate.

Immunohistochemistry

Tumor tissues was embedded in paraffin and cut into 4 μ m-thick sections. After heating in a microwave oven and blocking the antigen with 3% H₂O₂ solution, non-specific binding was blocked with 5% bovine serum albumin at 37°C for 30 minutes. Then the sections were incubated overnight at 4°C with the following primary antibody, RAC1 (Abcam, USA, 1:50). The signal was detected by the DAB method (Beyotime, China) and examined under a microscope (Nikon, Japan). The immunohistochemical staining score was evaluated by two pathologists. The scoring system used is as follows: no positive cells are

scored as 0; no positive cells are scored as 0. The yellow, light brown and dark brown staining of positive cells are 1-3 respectively. Each experiment was repeated three times.

Statistical analysis.

All statistical analyses were performed using SPSS 19.0 (SPSS, Chicago, IL, USA). Significant differences among two groups were compared using Student's t test. Comparisons among three or more groups were analyzed using ANOVA with post hoc Student–Newman–Keuls test. Statistical significance was considered at $P < 0.05$ and labeled with*.

Results

RAC1 negatively regulates miR-3613 in ovarian cancer cell

RAC1 was knocked down in SKOV3 cells to analyze whether this substrate regulates ovarian cancer through miRNA. After TRIzol (Invitrogen, USA) was used to extract total RNA and identify its quality, the expression changes of miRNA were analyzed on the Agilent microarray platform. A heat map was drawn by selecting 34 miRNAs with the most evident expression changes (Fig. 1A). qRT-PCR was then used to detect the expression of 13 differential miRNAs. MiR-3613 was found to be up-regulated most significantly after RAC1 knockdown (Fig. 1B). In addition, 20 pairs of ovarian cancer and adjacent tissues were chosen to detect miR-3613 expression. The results showed that the miR-3613 expression was higher in EOC than in normal tissues (Fig. 1C). Finally, 49 patients with ovarian cancer (Table 1) were equally grouped into two according to miR-3613 expression and then analyzed for survival. The results showed that patients with high miR-3613 expression had a long survival time (Fig. 1D). This finding indicates that RAC1 may promote the malignant progression of ovarian cancer by inhibiting miR-3613.

Table 1
Correlations between clinicopathological characteristics and has-miR-3613-5p expression in EOC patients

Variable	All cases	has-miR-3613-5p		P value
		Low expression	High expression	
Age				0.851
< 50	27	14	13	
≥ 50	22	12	10	
Tumor size (cm)				0.007**
< 5	20	6	14	
≥ 5	29	20	9	
FIGO stage				0.032*
I + II	24	9	15	
III + IV	25	17	8	
Histological grade				0.017*
Grade 1	21	7	14	
Grade 2–3	28	19	9	
Tumor type				0.518
Serous	34	17	17	
Non-serous	15	9	6	
Ascites (ml)				0.648
< 100	23	13	10	
≥ 100	26	13	13	
Serm CA125 (U/ml)				0.035*
< 35.0	22	8	14	
≥ 35.0	27	18	9	
*Statistically significant ($P < 0.05$), **Statistically significant ($P < 0.01$).				

miR-3613 inhibits ovarian cancer cell migration and proliferation

MiR-3613 overexpression plasmids were transfected in ovarian cancer cells OVCAR3 and SKOV3 to verify its role in ovarian cancer cells. The cells transfected with empty vector pcDNA3.1 were used as controls (Figure 2A). MTT and colony formation experiments were conducted for analysis. The results showed that miR-3613 overexpression inhibited cell viability (Figure 2B) and proliferation (Figure 2C). Transwell and wound healing assays were also performed to detect cell invasion and migration abilities, and the results showed that miR-3613 inhibited the invasion (Figure 2D) and migration (Figure 2E) of ovarian cancer cells and the expression of EMT-related markers N-cadherin and vimentin (Figure 2F).

miR-3613 directly targets RAC1

The roles of miRNA depend on downstream target genes. Prediction results revealed two miR-3613 binding sites in the 3'-UTR region of RAC1 (Figure 3A). Western blot analysis confirmed that miR-3613 repressed RAC1 expression (Figure 3B). Dual-luciferase reporter experiments were then conducted to verify the binding of miR-3613 to RAC1 mRNA. The fluorescent reporter vector carrying wild-type or mutant RAC1 mRNA was co-transfected with miR-3613 in OVCAR3 cells (Figure 3C). The findings showed that the fluorescence intensity of the group carrying wild-type RAC1 mRNA was inhibited by miR-3613 and then recovered after the mutation (Figure 3D). This result indicates that miR-3613 directly binds to RAC1 mRNA and inhibits the protein expression of RAC1. The expression of RAC1 mRNA and its correlation with miR-3613 were then analyzed in actual patients. RAC1 was found to be highly expressed in patients with ovarian cancer (Figure 3E) and was negatively correlated with miR-3613 (Figure 3F).

RAC1 reverses the inhibitory effect of miR-3613 in ovarian cancer cells

The above findings revealed the existence of the RAC1/miR-3613/RAC1 feedback loop. A rescue experiment to further confirm the role of this pathway in ovarian cancer. After miR-3613 was expressed in OVCAR3 and SKOV3 cells, RAC1 was overexpressed to test its expression and determine whether it could reverse the inhibitory effect of miR-3613. The results showed that the exogenous RAC1 transfection restored (Figure 4A) and even alleviated the inhibition of miR-3613 against cell viability (Figure 4B), proliferation (Figure 4C), migration (Figure 4D), and invasion (Figure 4E). Western blot results also showed that the expression of N-cadherin and Vimentin returned to normal after RAC1 expression was restored (Figure 4F).

MiR-3613 inhibits the tumor growth of ovarian cancer in vivo

Finally, the effects of RAC1 and miR-3613 tumor growth were verified in nude mice. First, a stable OVCAR3 cell line overexpressing miR-3613 was established. The mice were subcutaneously inoculated with these cells at a concentration of 6×10^5 per mouse. RAC1-overexpressing lentivirus was injected into the tumor with the maximum diameter of 0.5 cm. After the nude mice were euthanized, the solid tumors obtained from surgery were measured and then fixed with formaldehyde for subsequent immunohistochemical detection. The results showed that miR-3613 inhibited tumor growth, and RAC1 can reverse this inhibitory effect (Figures 5A and 5B). Immunohistochemical detection also confirmed that miR-3613 suppressed RAC1 expression in solid tumors (Figure 5C).

Discussion

Malignant tumors are usually characterized by metastasis, which leads to poor prognosis and limited therapeutic possibilities for patients with tumors. Metastasis is one of the coordination processes between tumor cells and their microenvironment during malignant progression, which includes invasion and migration[15, 16]. This step involves the active migration of tumor cells guided by integrins after matrix metalloproteinases degrade the extracellular matrix (ECM)[17]. The interaction between metastatic tumor cells and their ECM is essential for mediating the malignant phenotype. The ECM–integrin axis initiates and maintains important cellular functions and is an important regulator of tumor cell phenotype[18]. Rho GTPases contribute to different steps of cancer progression, including invasion and metastasis, and control signal transduction pathways. RAC1 is a small GTPase in the Rho family and mediates stimulus-induced (including integrin) actin cytoskeleton reorganization. Activated RAC1 acts as an intracellular signal transducer and regulates various cellular events, including cytoskeletal dynamics, to maintain cell morphology, polarity, adhesion, and migration. The extensive influence of RAC1 on tumor cell behavior has led to its potential as a therapeutic target [7, 19, 20]. In ovarian cancer, Rac1 knockdown can inhibit EMT progression and tumor growth in vivo by increasing E-cadherin and reducing vimentin[21, 22]. Here, we mainly focused on why ovarian cancer cells have persistent abnormal RAC1 expression and discovered the RAC1/miR-3613/RAC1 feedback loop. MiR-3613 inhibits the protein translation of RAC1, which in turn can achieve sustained expression by inhibiting miR-3613 expression. This finding served as a reminder that targeted therapy at the transcriptional and post-transcriptional levels of cancer-promoting genes appears to be indispensable.

EMT is a key aspect of tumor invasion and metastasis[23, 24]. Ovarian cancer is closely related to EMT, particularly during tumor development and peritoneal metastasis[25, 26]. RAC1 promotes EMT for many cancers [27–29]. An increased RAC1 activity can drive EMT in ovarian tumor cells. Inhibiting RAC1 activity or expression can restore the epithelial characteristics of ovarian tumor cells and prevent migration and invasion[21, 30–32]. MiRNA is a type of small non-coding RNA that controls the expression of target genes by inhibiting mRNA translation and inducing mRNA degradation. Many miRNAs regulate tumor invasion and metastasis through EMT-related mechanisms. In ovarian cancer, the EMT-inducing factor SNAI2 up-regulates PDCD10 by inhibiting miR-222-3p to induce EMT[33]. MiR-186 overexpression in ovarian cancer cells reduces Twist1 expression, thus making the cells highly sensitive to cisplatin in vitro and in vivo[34]. MicroRNA-150-5p promotes the EMT-mediated malignant progression of ovarian cancer by inhibiting c-Myb-mediated Slug suppression[35]. This study found that RAC1 can promote the EMT of ovarian cancer cells. MiR-3613 inhibits the protein translation of RAC1, which in turn suppresses the expression of miR-3613. This relationship allows ovarian cancer cells to continuously express RAC1 and promote the EMT and malignant progression of tumor cells.

In summary, a negative correlation was found between RAC1 and miR-3613 in ovarian cancer. RAC1 can maintain its continuous high expression in ovarian cancer cells by regulating miR-3613, thereby promoting malignant progression. This study is helpful to understand the mechanisms underlying the dysregulation of tumor-related genes and targeted drug development.

Declarations

Ethics approval and consent to participate: All procedures involving animals were approved by the Institutional Animal Care and Use Committee at the Shandong Provincial Hospital Affiliated to Shandong First Medical University.

Consent for publication: Not applicable

Availability of data and material: The datasets in this study are available from the corresponding author.

Competing interests: The authors declare no conflict of interest.

Funding: This study was funded by Shandong Natural Science Foundation (ZR2016HQ22) and Shandong Province Medical and Health Technology Development Project (2017ws191).

Authors' contributions: LRB responsible for cell experiments and writing, MYF and LN responsible for cell and animal experiments, LFF and ZYZ responsible for data analysis. LCZ conceived and designed the study.

Acknowledgment: Not Applicable

References

1. Cannistra SA (2004) Cancer of the ovary. *N Engl J Med* 351:2519–2529
2. Cooke SL, Brenton JD (2011) Evolution of platinum resistance in high-grade serous ovarian cancer. *Lancet Oncol* 12:1169–1174
3. Christie EL, Bowtell DDL (2017) Acquired chemotherapy resistance in ovarian cancer. *Ann Oncol* 28:viii13–viii15
4. Ledermann J, Harter P, Gourley C, Friedlander M, Vergote I, Rustin G, Scott CL, Meier W, Shapira-Frommer R, Safra T, Matei D, Fielding A, Spencer S, Dougherty B, Orr M, Hodgson D, Barrett JC, Matulonis U (2014) Olaparib maintenance therapy in patients with platinum-sensitive relapsed serous ovarian cancer: a preplanned retrospective analysis of outcomes by BRCA status in a randomised phase 2 trial. *Lancet Oncol* 15:852–861
5. Rossi L, Verrico M, Zaccarelli E, Papa A, Colonna M, Strudel M, Vici P, Bianco V, Tomao F (2017) Bevacizumab in ovarian cancer: A critical review of phase III studies. *Oncotarget* 8:12389–12405
6. Svensmark JH, Brakebusch C (2019) Rho GTPases in cancer: friend or foe? *Oncogene* 38:7447–7456
7. Jansen S, Gosens R, Wieland T, Schmidt M (2018) Paving the Rho in cancer metastasis: Rho GTPases and beyond. *Pharmacol Ther* 183:1–21
8. Abo A, Pick E, Hall A, Totty N, Teahan CG, Segal AW (1991) Activation of the NADPH oxidase involves the small GTP-binding protein p21rac1. *Nature* 353:668–670

9. Ridley AJ, Paterson HF, Johnston CL, Diekmann D, Hall A (1992) The small GTP-binding protein rac regulates growth factor-induced membrane ruffling. *Cell* 70:401–410
10. Bajanca F, Gougnard N, Colle C, Parsons M, Mayor R, Theveneau E (2019) In vivo topology converts competition for cell-matrix adhesion into directional migration. *Nat Commun* 10:1518
11. Aljaghtmi AA, Hill NT, Cooke M, Kazanietz MG, Abba MC, Long W, Kadakia MP (2019) DeltaNp63alpha suppresses cells invasion by downregulating PKCgamma/Rac1 signaling through miR-320a. *Cell Death Dis* 10:680
12. Hofbauer SW, Krenn PW, Ganghammer S, Asslaber D, Pichler U, Oberascher K, Henschler R, Wallner M, Kerschbaum H, Greil R, Hartmann TN (2014) Tiam1/Rac1 signals contribute to the proliferation and chemoresistance, but not motility, of chronic lymphocytic leukemia cells. *Blood* 123:2181–2188
13. Yao C, Yu KP, Philbrick W, Sun BH, Simpson C, Zhang C, Insogna K (2017) Breast cancer-associated gene 3 interacts with Rac1 and augments NF-kappaB signaling in vitro, but has no effect on RANKL-induced bone resorption in vivo. *Int J Mol Med* 40:1067–1077
14. Zoughlami Y, van Stalborgh AM, van Hennik PB, Hordijk PL (2013) Nucleophosmin1 is a negative regulator of the small GTPase Rac1. *PLoS One* 8:e68477
15. Hui L, Chen Y (2015) Tumor microenvironment: Sanctuary of the devil. *Cancer Lett* 368:7–13
16. Quail DF, Joyce JA (2013) Microenvironmental regulation of tumor progression and metastasis. *Nat Med* 19:1423–1437
17. Chiang AC, Massague J (2008) Molecular basis of metastasis. *N Engl J Med* 359:2814–2823
18. Brown NH (2000) Cell-cell adhesion via the ECM: integrin genetics in fly and worm. *Matrix Biol* 19:191–201
19. Pajic M, Herrmann D, Vennin C, Conway JR, Chin VT, Johnsson AK, Welch HC, Timpson P (2015) The dynamics of Rho GTPase signaling and implications for targeting cancer and the tumor microenvironment. *Small GTPases* 6:123–133
20. Smithers CC, Overduin M (2016) Structural Mechanisms and Drug Discovery Prospects of Rho GTPases, *Cells*. 5
21. Kenny HA, Chiang CY, White EA, Schryver EM, Habis M, Romero IL, Ladanyi A, Penicka CV, George J, Matlin K, Montag A, Wroblewski K, Yamada SD, Mazar AP, Bowtell D, Lengyel E (2014) Mesothelial cells promote early ovarian cancer metastasis through fibronectin secretion. *J Clin Invest* 124:4614–4628
22. Leng R, Liao G, Wang H, Kuang J, Tang L (2015) Rac1 expression in epithelial ovarian cancer: effect on cell EMT and clinical outcome. *Med Oncol* 32:329
23. Derynck R, Weinberg RA (2019) EMT and Cancer: More Than Meets the Eye. *Dev Cell* 49:313–316
24. Kalluri R, Weinberg RA (2009) The basics of epithelial-mesenchymal transition. *J Clin Invest* 119:1420–1428
25. Klymenko Y, Kim O, Stack MS (2017) Complex Determinants of Epithelial: Mesenchymal Phenotypic Plasticity in Ovarian Cancer, *Cancers (Basel)*. 9

26. Ottevanger PB (2017) Ovarian cancer stem cells more questions than answers. *Semin Cancer Biol* 44:67–71
27. Shin S, Buel GR, Nagiec MJ, Han MJ, Roux PP, Blenis J, Yoon SO (2019) ERK2 regulates epithelial-to-mesenchymal plasticity through DOCK10-dependent Rac1/FoxO1 activation. *Proc Natl Acad Sci U S A* 116:2967–2976
28. Kotelevets L, Chastre E (2020) Rac1 Signaling: From Intestinal Homeostasis to Colorectal Cancer Metastasis. *Cancers (Basel)*. **12**
29. He Y, Northey JJ, Pelletier A, Kos Z, Meunier L, Haibe-Kains B, Mes-Masson AM, Cote JF, Siegel PM, Lamarche-Vane N (2017) The Cdc42/Rac1 regulator CdGAP is a novel E-cadherin transcriptional co-repressor with Zeb2 in breast cancer. *Oncogene* 36:3490–3503
30. Guo Y, Kenney SR, Muller CY, Adams S, Rutledge T, Romero E, Murray-Krezan C, Prekeris R, Sklar LA, Hudson LG, Wandinger-Ness A (2015) R-Ketorolac Targets Cdc42 and Rac1 and Alters Ovarian Cancer Cell Behaviors Critical for Invasion and Metastasis. *Mol Cancer Ther* 14:2215–2227
31. Zhou G, Peng F, Zhong Y, Chen Y, Tang M, Li D (2017) Rhein suppresses matrix metalloproteinase production by regulating the Rac1/ROS/MAPK/AP-1 pathway in human ovarian carcinoma cells. *Int J Oncol* 50:933–941
32. Fang D, Chen H, Zhu JY, Wang W, Teng Y, Ding HF, Jing Q, Su SB, Huang S (2017) Epithelial-mesenchymal transition of ovarian cancer cells is sustained by Rac1 through simultaneous activation of MEK1/2 and Src signaling pathways. *Oncogene* 36:1546–1558
33. Fan L, Lei H, Zhang S, Peng Y, Fu C, Shu G, Yin G (2020) Non-canonical signaling pathway of SNAI2 induces EMT in ovarian cancer cells by suppressing miR-222-3p transcription and upregulating PDCD10. *Theranostics* 10:5895–5913
34. Zhu X, Shen H, Yin X, Long L, Xie C, Liu Y, Hui L, Lin X, Fang Y, Cao Y, Xu Y, Li M, Xu W, Li Y (2016) miR-186 regulation of Twist1 and ovarian cancer sensitivity to cisplatin. *Oncogene* 35:323–332
35. Tung CH, Kuo LW, Huang MF, Wu YY, Tsai YT, Wu JE, Hsu KF, Chen YL, Hong TM (2020) MicroRNA-150-5p promotes cell motility by inhibiting c-Myb-mediated Slug suppression and is a prognostic biomarker for recurrent ovarian cancer. *Oncogene* 39:862–876

Figures

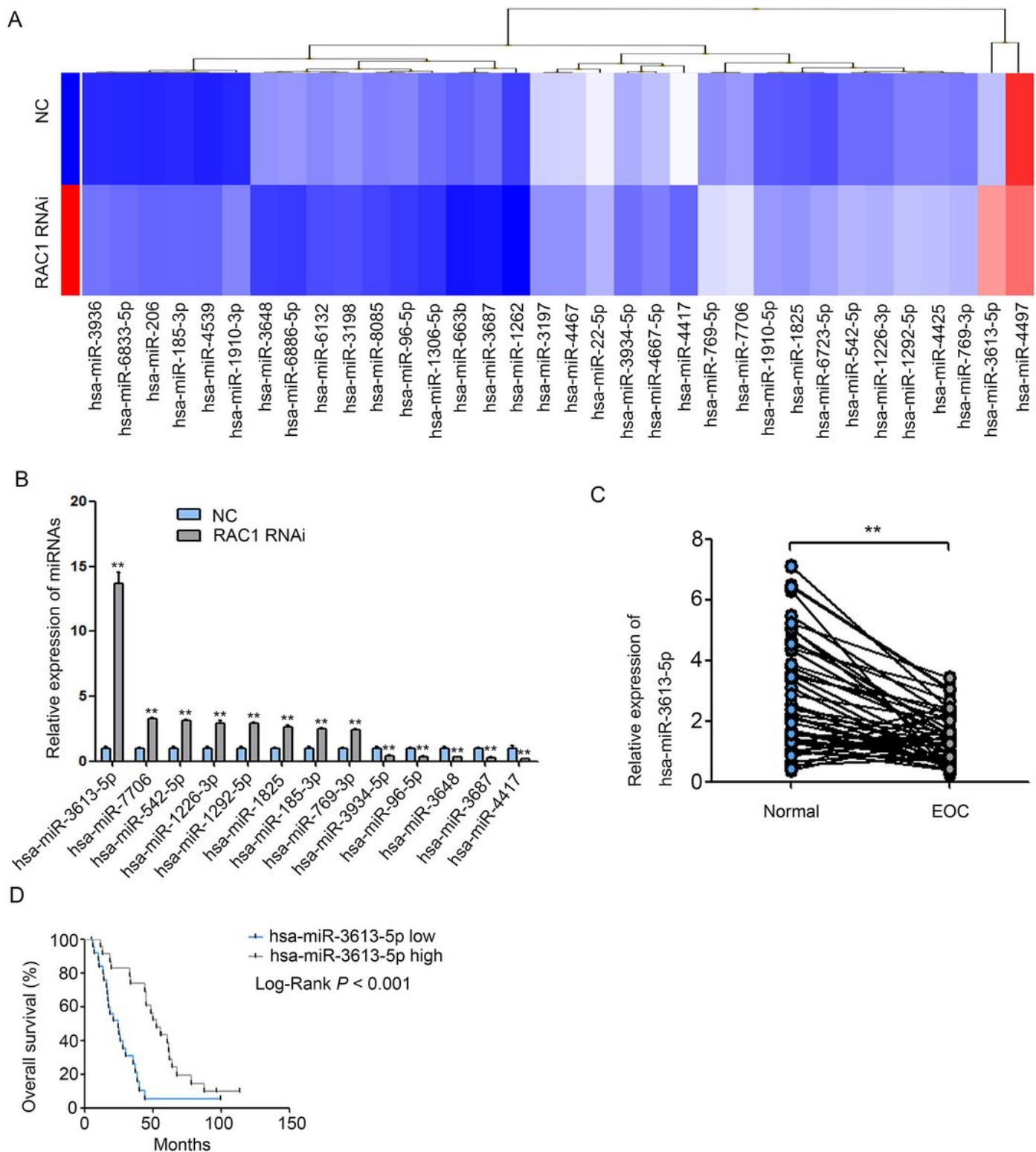


Figure 1

MiR-3613 is negatively regulated by RAC1 in ovarian cancer. A. After RAC1 knockdown in OVCAR3 cells, a heat map was constructed by selecting differential miRNAs through the microRNA array. B. Expression of 13 miRNAs detected by qRT-PCR in OVCAR3 cells after RAC1 knockdown. C. Expression of miR-3613 in epithelial ovarian cancer (EOC) and adjacent tissues. D. Overall survival rate of 49 patients with ovarian cancer and different miR-3613 expression levels.

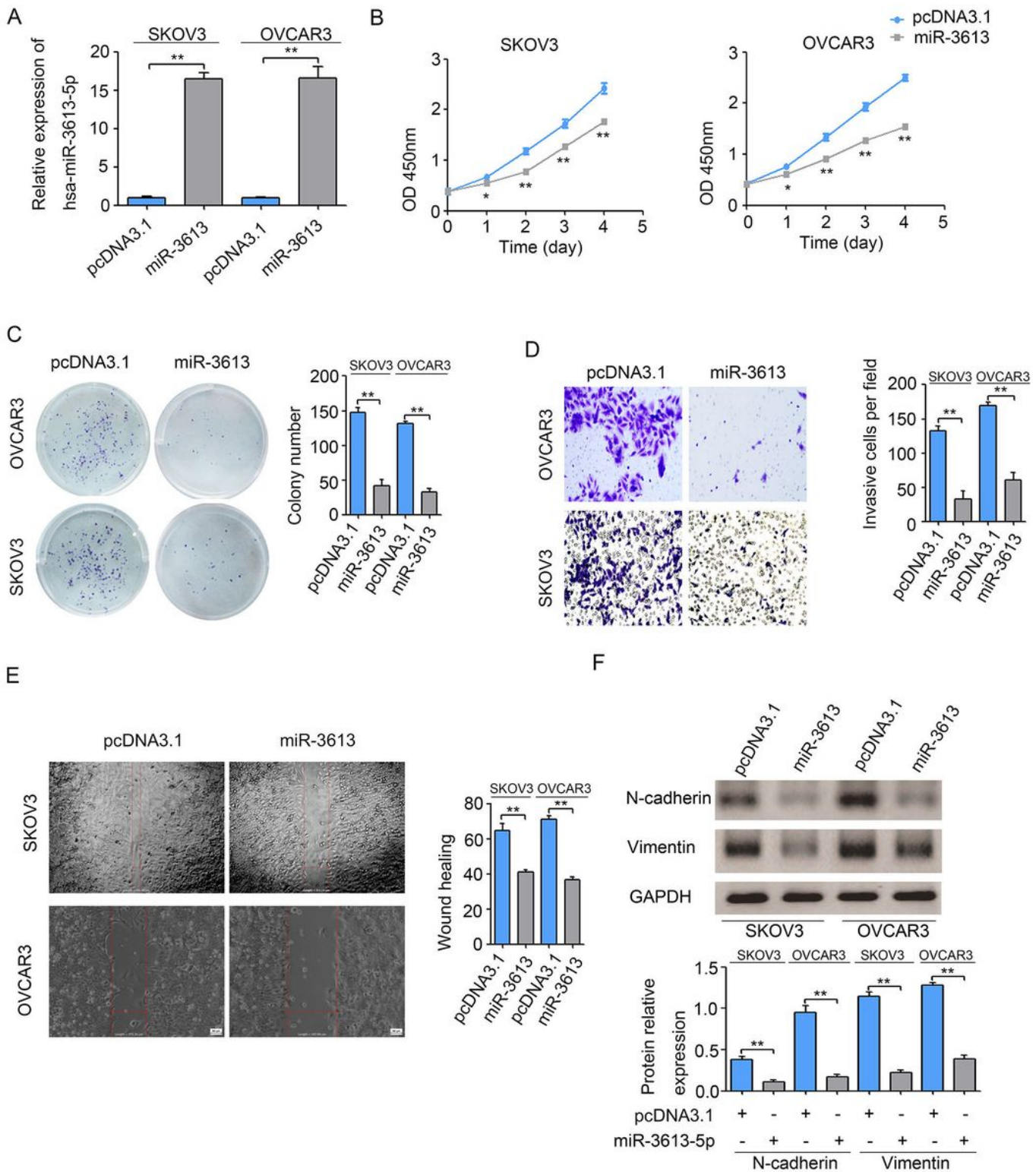


Figure 2

MiR-3613 inhibits the invasion and migration of ovarian cancer cells. Ovarian cancer cells SKOV3 and OVCAR3 were transfected with miR-3613 expression plasmids, with pcDNA3.1 used as the control. A. After 48 hours, miR-3613 expression was detected by qRT-PCR. B. MTT assay was performed to analyze cell viability. C. Colony formation was used to detect cell proliferation. D. Cell invasion ability was

analyzed by transwell assay. E. Cell migration was detected by wound healing assay. F. Expression of EMT markers N-cadherin and vimentin was examined by Western blot.

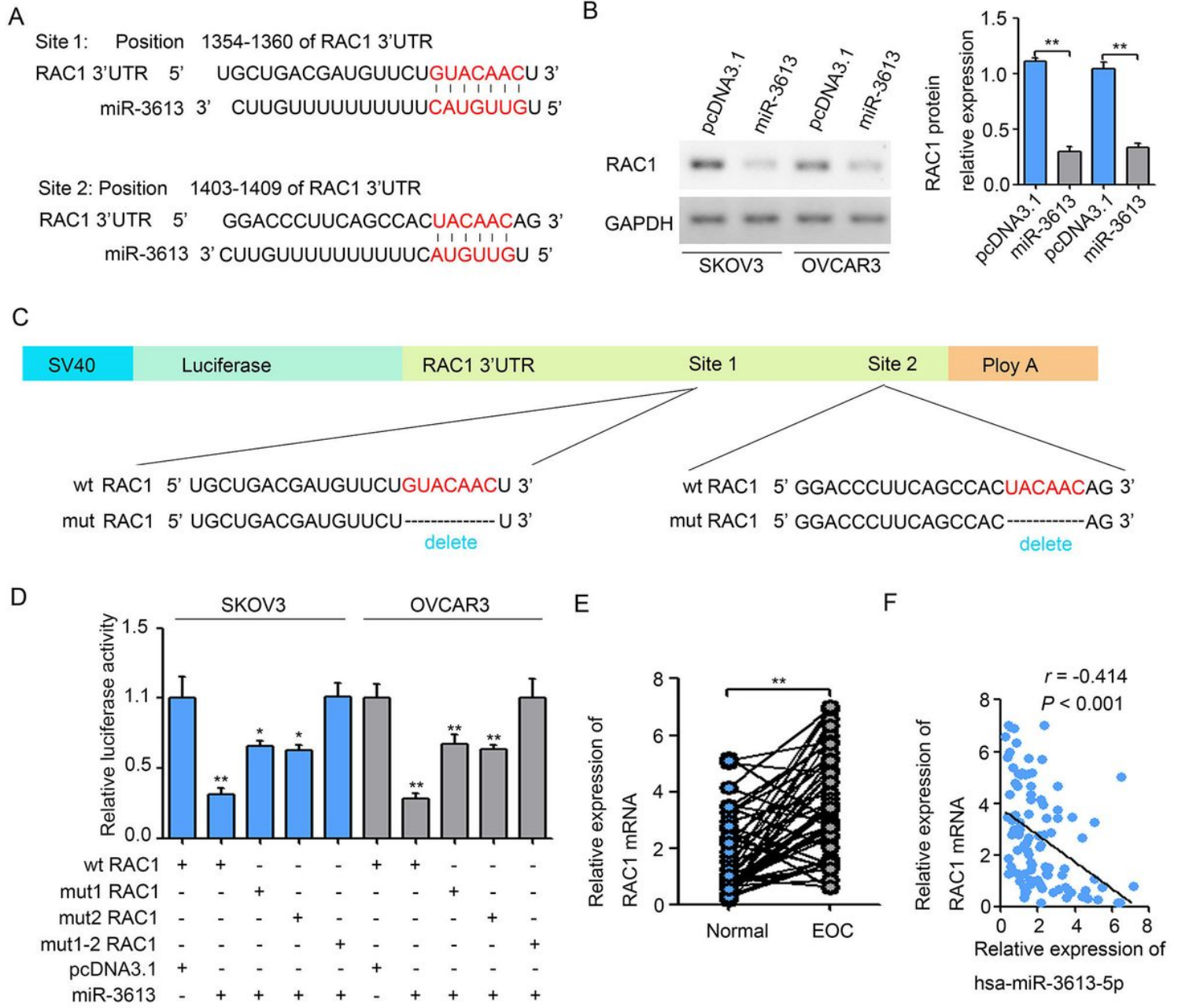


Figure 3

MiR-3613 directly targets RAC1. A. MiR-3613 binding sites in RAC1 mRNA 3'UTR. B. RAC1 protein levels after miR-3613 overexpression in ovarian cancer cells SKOV3 and OVCAR3. C. Wild and mutated RAC1 3'UTR inserted into pmirGLO dual-luciferase report vector. D. MiR-3613 and luciferase report vector with wt RAC1 3'UTR/mut RAC1 3'UTR co-transfected in OVCAR3 cells. Luciferase activity was analyzed after 48 hours. E. RAC1 mRNA levels in clinical specimens of EOC and normal tissues. F. Correlation between RAC1 and miR-3613 expression in patients with EOC.

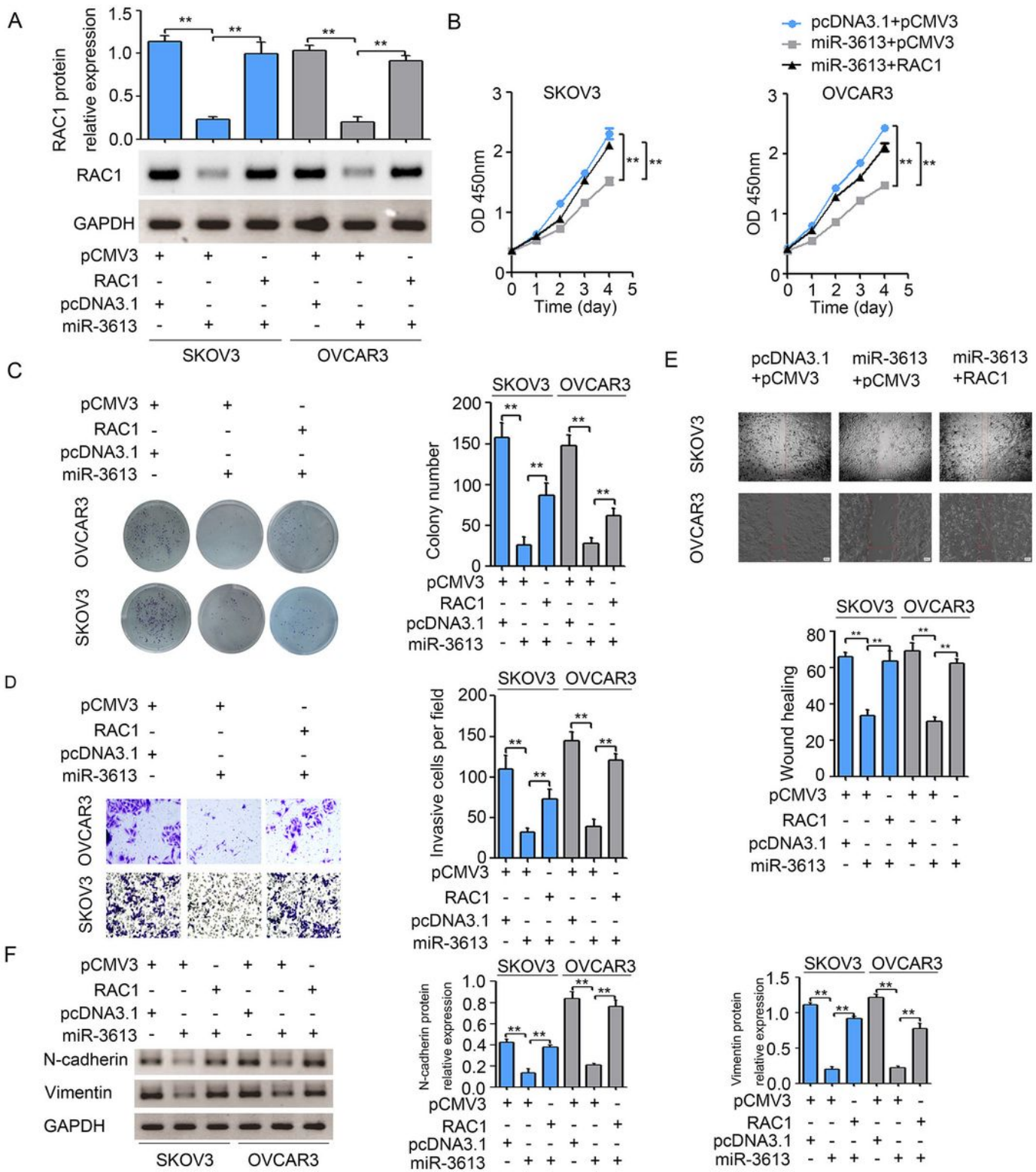


Figure 4

RAC1 counteracts the inhibitory effect of miR-3613 in ovarian cancer cells. After overexpressing miR-3613 alone or with RAC1 in ovarian cancer cells, the ability of RAC1 to reverse the inhibitory effect of miR-3613 on ovarian cancer cells was determined. A. After 48 hours, Western blot was used to detect RAC1 protein level. B. Cell viability was analyzed by MTT assay at different time points. C. Colony formation assay was performed to detect cell proliferation. D&E. Wound healing and transwell assay were used to

analyze cell migration and invasion ability. F. Protein levels of N-cadherin and vimentin were detected by Western blot.

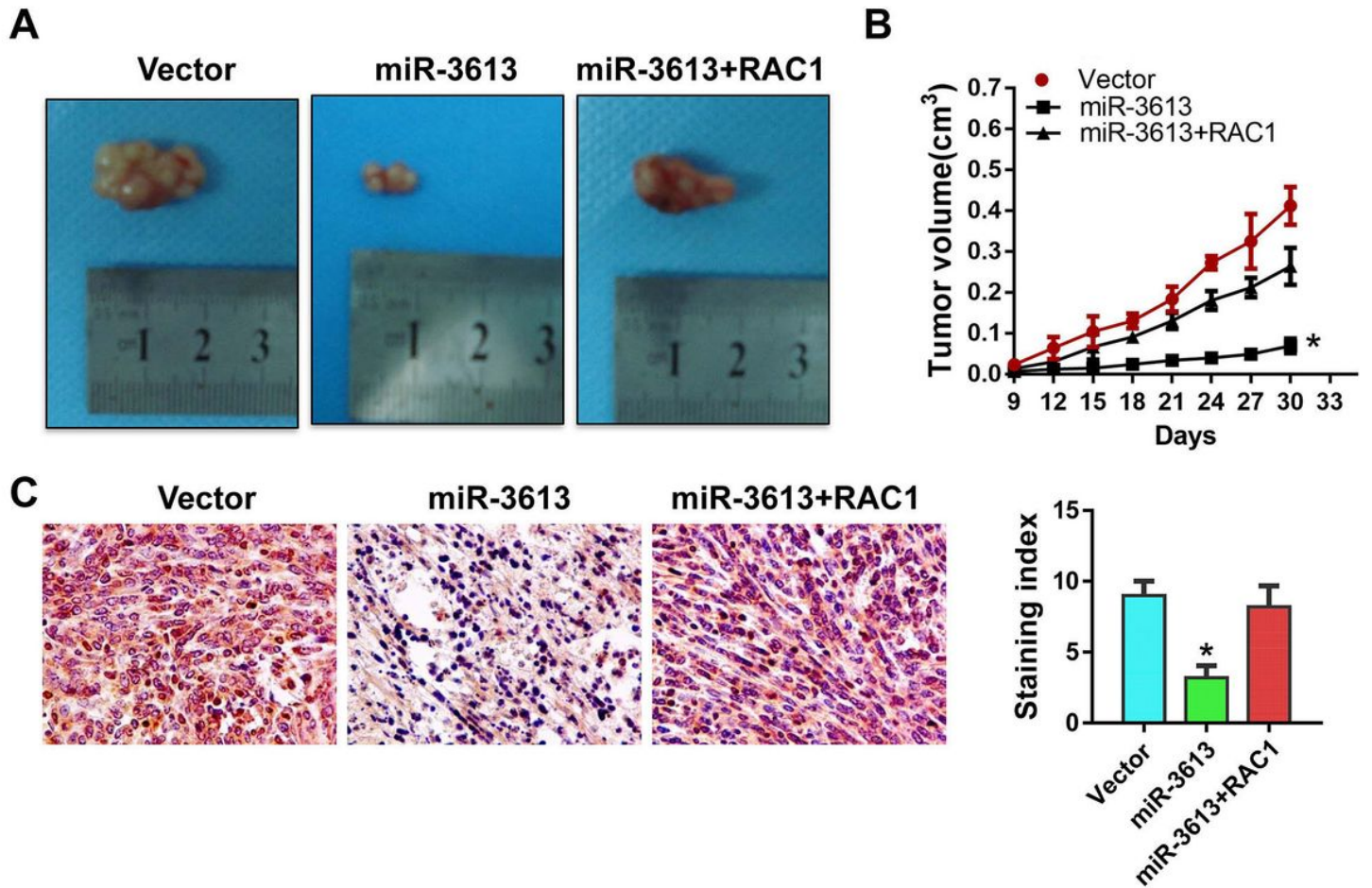


Figure 5

RAC1 reverses the effect of miR-3613 on ovarian cancer in vivo. After the OVCAR3 stable cell line overexpressing miR-3613 was injected subcutaneously into nude mice and the tumors had formed, the animals were injected with lentivirus overexpressing RAC1. The solid tumor obtained from surgery was measured and then fixed, and IHC was used to detect RAC1 expression. A. Solid tumors after mice were sacrificed. B. Tumor volume of each group. C. IHC was performed to detect RAC1 expression in these solid tumor tissues.